

Determination of Diffusion Coefficient of a Small Hydrophobic Probe in Poly(lactide-co-glycolide) Microparticles by Laser Scanning Confocal Microscopy

Jichao Kang and Steven P. Schwendeman*

Department of Pharmaceutical Sciences, The University of Michigan, Ann Arbor, Michigan 48109-1065

Received July 1, 2002; Revised Manuscript Received November 12, 2002

ABSTRACT: The diffusion coefficient of a small hydrophobic probe in poly(lactide-co-glycolide) (PLGA) microparticles was determined by laser scanning confocal microscopy (LSCM). PLGA microparticles preincubated in a physiological buffer for various times were immersed in an aqueous solution of the pH-insensitive fluorescent probe bodipy at 37 °C. Probe concentration gradients inside individual microparticle matrices were then recorded by LSCM, which were accurately fit by the solution to Fick's second law of diffusion to determine an effective probe diffusion coefficient (D) in the polymer matrix. Values of D varied less than expected from the blank eroding polymer and were in the range $(3-10) \times 10^{-12}$ cm²/s. The apparent polymer-water partition coefficient of the probe was also determined to be roughly 20, indicative of strong partitioning into the polymer phase. The diffusion of bodipy in microparticles varied over 3 orders of magnitude between 22 and 43 °C, indicative of transport control in the polymer phase as opposed to a pore diffusion mechanism. The diffusion model also predicted exceptionally well the release of probe encapsulated in microparticles when a time-averaged D , which had been determined in blank microparticles by LSCM, was used. Values of D for bodipy in PLGA microparticles encapsulating bovine serum album were of similar value $((3-24) \times 10^{-12}$ cm²/s) but better reflected the multiphasic behavior characteristic of PLGA erosion. The LSCM method described here is simple, nondestructive, and accurate and can be used to study the diffusion inside a single polymer microparticle.

Introduction

Biomaterials prepared from copolymers of lactic and glycolic acids (PLGA) are currently among the most commonly used in medicine.¹⁻⁵ PLGA particulate systems, including nanospheres/particles and microspheres/particles/capsules and the like, have been shown to be extremely popular and powerful tools in drug and vaccine delivery technologies as well as diagnostic imaging.^{4,6,7} Despite their widespread use, the number of reports characterizing the fundamental transport of small and large molecules in these polymers has been surprisingly few.⁸⁻¹⁰ Several difficulties in such measurements include the small length scale of microparticulates, the multiple processes contributing to transport,⁹ and the time-dependent changes in the physical-chemical state of the PLGA during polymer erosion.^{11,12} Transport studies could be particularly valuable for understanding the release kinetics of the encapsulated substances and the acidic water-soluble monomers and oligomers produced during hydrolytic degradation of the polymer. Moreover, partitioning and transport of molecules from the surrounding biological milieu into PLGA implants has been suggested as a possible source for observed differences in the rates of polymer degradation in vivo and in vitro.¹³

Pathways contributing to molecular transport in PLGA systems can be grouped into diffusion, erosion (i.e., mass loss), and osmotically mediated events.¹⁴ For release of proteins, which are dispersed within aqueous pores throughout the polymer matrix, either of the three pathways can potentially play an important role and diffusion occurs through aqueous pores. For small

hydrophobic drugs, which strongly partition into the polymer phase, diffusion in the polymer phase is expected unless one of the aforementioned pathways were to become dominant (e.g., following the induction phase when polymer mass is rapidly released).^{11,12} Of these important processes, this paper focuses on diffusion in the polymer phase.

A description of several techniques for diffusion coefficient measurement can be found elsewhere.¹⁵⁻²¹ These techniques include (1) permeation or diaphragm cell methods, (2) uptake/release methods, (3) methods based on determination of the concentration profile, and (4) instrumental methods. Among these methods, concentration-profile-based methods would appear to be most useful for monitoring diffusion in biodegradable microparticles, since the first method requires a membrane, the second is complicated by poor discrimination of transport mechanisms, and the fourth often imposes some restriction on the systems that can be studied.

For example, the concentration-profile-based method, which employs laser scanning confocal microscopy (LSCM), has recently been used to study diffusion in both solutions and polymers.²²⁻²⁴ Song²⁵ used LSCM to study dye diffusion in nylon-66 fibers and found the diffusion coefficient measured by LSCM agreed well with values obtained from traditional destructive techniques. Sasaki²⁶ used laser trapping microspectroscopy and LSCM to measure in situ the ion-exchange processes in single cation-exchange resin particle. De Smedt et al.²⁷ and Burke et al.²⁸ measured the diffusion coefficients of macromolecules in gel and solution by fluorescence recovery after photobleaching (FRAP) using LSCM.

In the present study, we determined the diffusion coefficient of a small and pH-insensitive hydrophobic

* To whom correspondence should be addressed: phone (734) 615-6574; FAX (734) 615-6162.

probe in PLGA microparticles by taking advantage of the optical slice and high-resolution image capability of LSCM. Since the PLGA physical-chemical properties are time-dependent during polymer erosion, this technique relied on the assumption that diffusion of the probe was fast relative to changes in the polymer. Both this assumption and the LSCM technique were validated, and the diffusion coefficient in blank PLGA microparticles was determined as a function of time and temperature and compared with values obtained from PLGA microparticles encapsulating protein.

Experimental Section

Materials. Poly(DL-lactide-co-glycolide) 50/50, end group capped, with an inherent viscosity of 0.19 dL/g in HFIP at 30 °C was obtained from Birmingham Polymers, Inc. (Birmingham, AL). Bodipy, FL (Bodipy, MW 292.1, $P_{\text{octanol/water}} = 0.9$), was from Molecular Probes, Inc. (Eugene, OR). Poly(vinyl alcohol) (PVA) (80% hydrolyzed, MW 9–10 kDa) was from Aldrich Chemical Co., Inc. (Milwaukee, WI). Bovine serum albumin (BSA) and magnesium carbonate were from Sigma Chemical Co. (Louis, MO). All other reagents were analytical grade or higher and used as received.

Preparation of Blank PLGA Microparticles. PLGA microparticles were prepared by a water-in-oil-in-water double emulsion-solvent evaporation method.^{2,3} Briefly, 100 μ L of PBS (8 mM Na_2HPO_4 , 1 mM KH_2PO_4 , 137 mM NaCl, 3 mM KCl, pH 7.4) solution was added to 1 mL of 700 mg/mL PLGA in methylene chloride solution and homogenized at 10 000 rpm for 1 min with a Tempest IQ² homogenizer (The VirTis Co., Gardiner, NY) equipped with a 10 mm shaft to make the first emulsion. One milliliter of 2% PVA solution was then added to the emulsion, and the mixture was immediately vortexed (Genie 2, Fisher Scientific Industries, Inc., Bohemia, NY) for 20 s to make the final emulsion. The resultant emulsion was added to 100 mL of 0.5% PVA solution, and the methylene chloride was evaporated for 3 h under stirring. Hardened microparticles were collected by centrifugation and washed three times with purified water and finally freeze-dried. For freeze-drying, samples were flash frozen in liquid nitrogen and placed on a Freezone 6 freeze-drying system (Labcono, Kansas City, MO) at 133×10^{-3} mbar or less with a condenser temperature of -46 °C for 48 h.

Encapsulation of BSA and Bodipy in PLGA Microparticles. BSA- and bodipy-encapsulated PLGA microparticles were also prepared by the above method using an internal phase containing either 300 mg/mL BSA or 20 μ g/mL bodipy in PBS solution. PLGA microparticles containing both MgCO_3 and BSA were prepared by adding 3% MgCO_3 into PLGA/ CH_2Cl_2 solution and using 300 mg/mL BSA solution as the internal phase. Bodipy microparticles were sieved (U.S.A. standard sieve series, sieve No. 325 and 635, Newark Wire Cloth Co, Newark, NJ), and only those between 20 and 45 μ m were collected for freeze-drying and further characterization.

Surface Characterization and Size Distribution of PLGA Microparticles by Scanning Electron Microscopy (SEM). PLGA microparticles were first coated with gold for 200 s by a Vacuum Coater (Desk II, Denton Vacuum, Inc., Hill, NJ). The microparticle morphology was observed by a scanning electron microscope (S3200N variable pressure SEM, Hitachi), and the voltage was set at 15 keV. For size distribution analysis, the sizes of more than 200 particles were measured from micrographs.

Constant Temperature Incubation of PLGA Microparticles and Probe Uptake. PLGA microparticles were incubated under physiological conditions for various times before monitoring the probe uptake. About 1 mg of PLGA microparticles was incubated at 37 °C in 1 mL of PBS containing 0.02% (w/v) Tween-80 (PBST) under mild agitation (by a KS 125 basic shaker, IKA labortechnik, Germany) for predetermined times. After incubation, the microparticles were separated from PBST solution by a brief centrifugation. Then, 1 mL of bodipy in PBST (5 μ g/mL), which was preincubated

at 37 °C, was added, and the mixture was incubated at 37 °C for various times (1 h–3 days) under mild agitation before LSCM observation.

Monitoring Probe Distribution in PLGA Microparticles by LSCM. A Carl Zeiss LSM 510 (Car Zeiss Microimaging, Inc., Thornwood, NY) laser scanning confocal microscope was used to observe the probe distribution in microparticles. The instrument was equipped with four laser systems, an Ar laser (458, 488, 514 nm, 25 mW), a HeNe 1 laser (543 nm, 1 mW), a HeNe laser 2 (633 nm), and an Enterprise laser (351, 364 nm), a photomultiplier (PMT), and a computer for image building and instrument control. The connected microscope was a Carl Zeiss inverted Axiovert 100 M that was fully motorized and could be operated via the LSM 510 software. The 488 nm line of the Ar ion laser and LP 505 filter was used in conjunction with a C-Apochromat 63 \times N.A. 1.2 water immersion objective lens to build images. Unless otherwise stated, the laser was set at 1.25% of the 25 mW (300 μ W) full power, and the detection gain was set at 750. The pinhole was set at 67 μ m, which resulted in an optical slice of less than 0.6 μ m. The laser was focused in the center of a microsphere, and a 512×512 pixels image was scanned at a scan speed of 1.12 μ s/pixel. Only microparticles with diameters between 30 and 40 μ m were imaged.

Image and Data Analysis. The image scanned by LSCM was analyzed either by LSM 510 or Scion Image software (Scion Corp., Frederick, MD). First, 4–8 intensity profiles along the diameter were obtained by the profile function of the software, which were then averaged to get the pixel intensity-position data pairs. Then the data were input into a spreadsheet software, in which the intensity (I)-position (r) data pairs were normalized by the surface intensity (I_0) and radius (a) of the microsphere, respectively, to get the $I/I_0-r/a$ data pairs (which is equivalent to $C/C_0-r/a$ pairs). The $C/C_0-r/a$ pairs were then fit by the following solution²⁹ to Fick's second law of diffusion for a constant probe source at a microsphere surface:

$$\frac{C}{C_0} = \frac{1}{r/a} \sum_{n=0}^{\infty} \left(\operatorname{erfc} \frac{(2n+1) - r/a}{2\sqrt{Dt/a^2}} - \operatorname{erfc} \frac{(2n+1) + r/a}{2\sqrt{Dt/a^2}} \right) \quad (1)$$

where t is time and D is the effective diffusion coefficient in the polymer matrix. C and C_0 are the probe concentration inside the polymer matrix and at the surface, respectively. The fitting was carried out according to a least-squares nonlinear regression using $n = 12$ (DataFit, Oakdale Engineering, Oakdale, PA) to obtain the values of D . Using values larger than $n = 12$ did not change the fitted value of D .

Temperature Dependence of Bodipy Diffusion in PLGA Microparticles. PLGA microparticles with or without protein were incubated in PBST at 37 °C for 5 days and subsequently equilibrated at 4.0, 22.5, 31.0, 37.0, or 43.0 °C for 3 h. A aliquot of 5 μ g/mL bodipy in PBST, which had been equilibrated at the same temperature as the microparticles, was then added to the microparticle suspension, and the mixtures were incubated at the same temperature for certain time periods (lower temperature required longer time) before the confocal image analysis and calculation of diffusion coefficients.

HPLC Analysis of Bodipy Samples. A Waters HPLC system was used for bodipy analysis. It consisted of a 1525 binary pump, a 717 plus autosampler, and a 474 scanning fluorescence detector. A 50 μ L sample of bodipy was injected into an ODS column fitted with a guard column (Nova-Pak C₁₈, Waters) and eluted with a mobile phase of 90% (v/v) methanol in phosphate buffer (0.02 M KH_2PO_4 with 0.02% triethylamine, pH 5.9) solution. Bodipy was detected by a fluorescence detector ($\lambda_{\text{ex}}/\lambda_{\text{em}} = 495/515$ nm, Gain 100, attenuation 1 and response 5 s). The flow rate was set at 1 mL/min, which resulted in a retention time of 2.8 min.

Loading and Encapsulation Efficiency of Bodipy Encapsulated PLGA Microparticles. Five milligrams of bodipy-PLGA microparticles was dissolved in 1 mL of a 90:

10 (v/v) acetonitrile–water mixture. The solution was then diluted and analyzed by HPLC. Drug loading (drug weight/microparticle weight) and encapsulation efficiency (actual loading/theoretical loading) were then calculated.

Bodipy Release from PLGA Microparticles. Five milligrams of bodipy–PLGA microparticles was suspended in 2 mL of PBST solution and incubated at the same condition used for probe uptake (37 °C, mild agitation). At predetermined times, microparticles were briefly centrifuged, and release media were replaced with preincubated fresh PBST. The release was then analyzed by HPLC.

PLGA/PBST Partition Coefficient. The partition coefficient of bodipy in PLGA was estimated by a depletion method.³⁰ Ten milligrams of blank PLGA microparticles (W_1) was incubated with 1 mL of 1, 5, and 10 $\mu\text{g/mL}$ bodipy in PBST solution (aqueous phase weight $W_2 = 1$ g) at 37 °C for 4 days. Bodipy solutions without microparticles were also incubated for control. The apparent partition coefficient (K_{app}) was calculated from the initial and equilibrium drug concentration (C_0 and C_e , respectively) in the media using (2):

$$K_{\text{app}} = \frac{W_2(C_0 - C_e)}{W_1 C_e} \quad (2)$$

Predicting Bodipy Release from PLGA Microparticles. Because of the very low loading of probe in PLGA (i.e., below probe solubility in the polymer phase), probe release can be predicted by the equation for drug release from a monolithic solution. The release medium was also frequently changed to guarantee the sink conditions. Therefore, the release is virtually the inverse process of the uptake study. Crank's solution for the release from spherical geometry under these conditions is as follows:²⁹

$$\frac{M_t}{M_\infty} = 1 - \sum_{n=1}^{\infty} \frac{6}{\pi^2 n^2} \exp(-Dn^2 \pi^2 t/a^2) \quad (3)$$

For particles with heterogeneous size distribution, (3) was modified as follows by addition of the fractional release from each particle in the size distribution:

$$\frac{M_t}{M_\infty} = \sum_{i=1}^m V_i \left(1 - \sum_{n=1}^{\infty} \frac{6}{\pi^2 n^2} \exp(-Dn^2 \pi^2 t/a_i^2) \right) \quad (4)$$

where m is the total number of particles; a_i and V_i are the radius and fractional volume of the i th individual particle of the particle population. The D determined for blank microparticles was used together with (3) and (4) to predict the release profile of bodipy microparticles.

Results and Discussion

Validation of pH-Insensitive Dye, Bodipy, for Probe Diffusion Studies. Commonly used fluorescent probes such as fluorescein and rhodamine are pH-sensitive, which compromises their use for drug transport experiments in the variable pH microclimate of the PLGAs.^{22,25} Therefore, we employed a pH-insensitive, hydrophobic probe, bodipy, in the present study, which has been reported to exhibit a negligible fluorescent intensity change over a pH range of 2–10.³¹ As shown in Figure 1A, little variation in the fluorescent intensity is exhibited over a broad range of pH.

The basis on which LSCM can be used for quantitative measurement is the linear fluorescence intensity–probe concentration relation. The primary causes for the deviation from linearity include fluorescence saturation, inner filter effect, and reabsorption.^{32–34} Fluorescence saturation occurs when the exciting illumination is so intense that a significant fraction of the fluorophore is no longer able to respond to the incident intensity. In

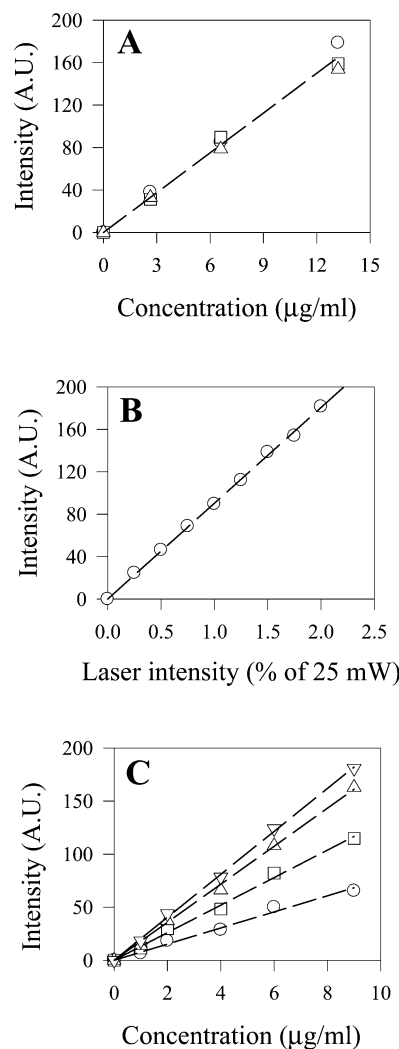


Figure 1. Validation of LSCM for probe diffusion studies. The gain was set at 750 with a laser intensity of 300 μW unless otherwise stated. (A) The fluorescence intensity (arbitrary units) of bodipy at pH 2.3 (Δ), 4.5 (\square), and 7.4 (\circ). (B) The linear relationship between fluorescence intensity and laser intensity. (C) Dependence of fluorescence intensity on probe concentration. The gain setting for the PMT was 700 (\circ), 750 (\square), 770 (Δ), and 790 (∇). The trend lines had $R^2 > 0.99$.

our experiments, only 1.25% of the full laser power (300 μW) was used to ensure that the saturation threshold was not reached. This was confirmed by the linear relationship between fluorescent intensity and laser intensity, as shown in Figure 1B. Inner filter effects and reabsorption occur when the probe concentration is too high. In our probe uptake experiments to follow, a low concentration of probe (5 $\mu\text{g/mL}$) was used in order to prevent the deviation of the intensity–concentration relation from the linear curve. In Figure 1C, linear emission intensity–concentration relationships are displayed at various gain settings, which cover the relevant conditions for uptake studies.

Monitoring Probe Uptake in PLGA Microparticles. A scanning electron micrograph of blank PLGA microparticles is shown in Figure 2. PLGA microparticles were spherical with a smooth surface and sporadically distributed small pores. When microparticles are immersed in an aqueous solution, the uptake process can be considered to occur in three steps.²⁵ First, probe molecules diffuse from the solution to the surface of microparticles. Second, probe molecules partition onto

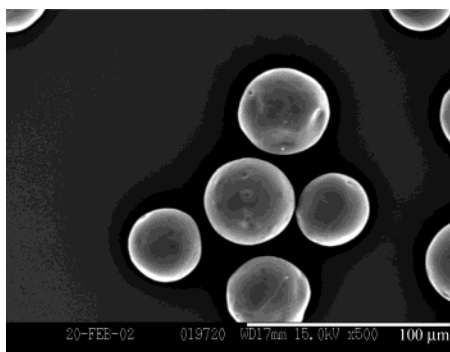


Figure 2. Scanning electron micrograph of blank PLGA microparticles used for diffusion coefficient measurement.

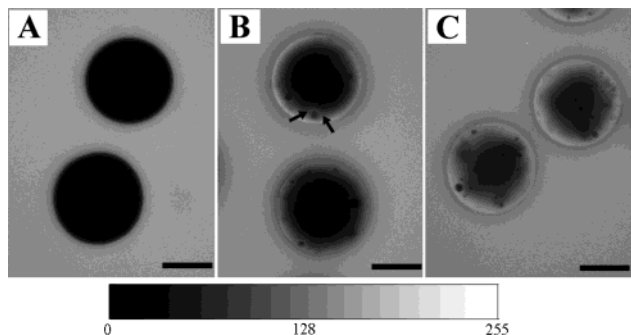


Figure 3. LSCM micrographs of the fluorescent intensity gradients in PLGA microparticles, which had undergone 14 days of erosion and then 1.5 (A), 5 (B), and 11 h (C) of probe diffusion under physiological conditions. The scale bars represent 20 μm . The arrow points to a region of the microparticles that the diffusion front has been advanced by an aqueous pore.

the surface of polymer matrix. And third, probe molecules diffuse inside the microparticles with a net transport toward the particle center. Because of the highly restricted transport in PLGA,^{30,35} probe diffusion inside the polymer matrix can be assumed to be the rate-limiting step and diffusion of probe in solution and partitioning into the microparticle surface are assumed to occur comparatively fast. By using a large amount of solution relative to polymer, another assumption can be made that probe concentration in the surface of microparticles is constant (C_0) during the entire incubation time, i.e., the infinite source condition. By determination of the probe concentration gradient ($C/C_0 - r/a$) inside microparticles, the solution to Fick's second law of diffusion (see (1)) can be fitted to the experimental concentration profiles to determine D .

In Figure 3, the kinetics of probe uptake in blank PLGA microparticles that were preincubated for 14 days in PBST at 37 $^{\circ}\text{C}$ is viewed by LSCM. The emitted fluorescence by the probe occupied a steadily increased fraction of the microparticles with time of incubation. The small dark spots in the probe-occupied area inside the microparticles correspond to aqueous pores in the microparticles. These regions were less bright than in the polymer because the probe concentration in polymer is much higher. Adjacent to such isolated pores could be observed frequently an advancement of the diffusion front (see thin emission line between the microparticle center and the pore designated by the arrow in Figure 3), since the diffusion across the aqueous pores is rapid relative to diffusion in the polymer phase. Examples of the concentration profiles of the probe across the microparticles after 1.5, 5, and 11 h of diffusion at 37 $^{\circ}\text{C}$

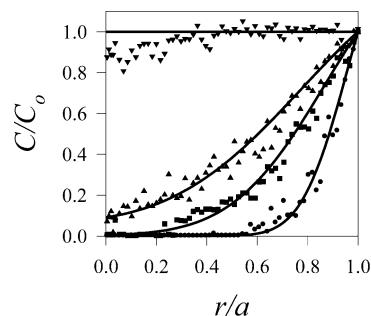


Figure 4. Examples of measured and fitted probe concentration profiles inside PLGA microparticles after 1.5, 5, and 11 h of probe uptake. An equilibrium line is drawn through the 3 day probe incubation data. Microparticles were incubated in PBST for 14 days before the probe uptake. The calculated D from 1.5 (\bullet), 5 (\blacksquare), and 11 h (\blacktriangle) of probe uptake was $(6.7 \pm 2.0) \times 10^{-12}$, $(6.5 \pm 1.3) \times 10^{-12}$, and $(5.7 \pm 1.2) \times 10^{-12} \text{ cm}^2/\text{s}$ (mean \pm SD, $n = 5$), respectively.

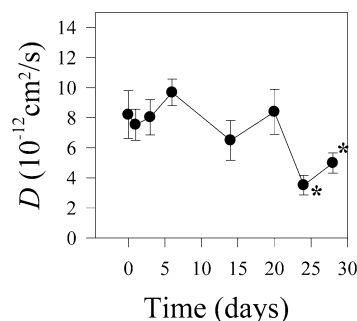


Figure 5. Diffusion coefficients of bodipy in blank PLGA microparticles as a function of erosion time in PBST at 37 $^{\circ}\text{C}$ (mean \pm SD, $n = 10$). Probe diffusion was recorded after 5 h. (*) Substantial microparticles formed aggregates. Values of D were measured from the nonaggregated particles.

and the curves fitted to (1) are shown in Figure 4. The concentration profile in the microparticles after equilibrium (3 days) is also shown. The excellent fit to the data ($R^2 > 0.90$) and the fact that D did not change over the several hour time interval (i.e., fitted $D = 6.7 \times 10^{-12}$, 6.5×10^{-12} , and $5.7 \times 10^{-12} \text{ cm}^2/\text{s}$ at 1.5, 5, and 11 h) indicated the validity of the diffusion model for the probe diffusion in PLGA microparticles.

Influence of Polymer Erosion Time and Protein Encapsulation on Probe Diffusion. After preincubation in PBST at 37 $^{\circ}\text{C}$ for predetermined periods of time, PLGA microparticles were immersed into a bodipy solution for 1.5–5 h, and the diffusion coefficients were calculated, as shown in Figures 5 and 6. Although the physical–chemical properties of PLGA during erosion are time-dependent, it is reasonable to assume that diffusion coefficients are virtually constant in the short uptake period, consistent with the fits described in Figure 4. For blank microparticles, the fits were excellent (R^2 invariably > 0.90) when incubated in PBST for less than 20 days. For longer incubation, particle aggregates appeared, and the remaining nonaggregated microparticles showed irregular shape and increased aqueous pores close to the surface, which led to a more heterogeneous probe distribution ($R^2 > 0.85$).

The diffusion coefficients of bodipy in blank microparticles ranged from 3.5×10^{-12} to $9.7 \times 10^{-12} \text{ cm}^2/\text{s}$. This value is similar to the diffusion coefficient of progesterone in poly(DL-lactic acid) determined by the diffusion cell method by Pitt et al. ($5.1 \times 10^{-12} \text{ cm}^2/\text{s}$).³⁰ The diffusion coefficients for this relatively hydrophobic

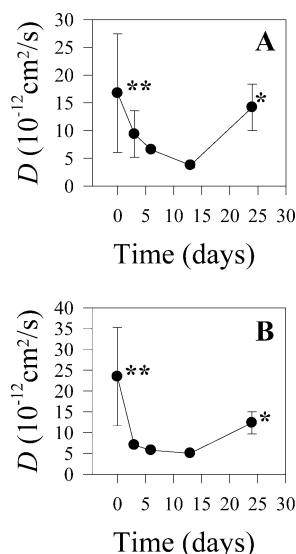


Figure 6. Diffusion coefficients of bodipy in protein-encapsulated PLGA microparticles in the absence (A) or presence of 3% MgCO₃ (B) as a function of erosion time in PBST at 37 °C (mean \pm SD, $n = 10$). Probe diffusion was recorded after 5 h. (**) Values for D at initial time points were highly variable due to heterogeneous probe distribution and irregular shape of the microparticles after probe uptake. (*) Substantial microparticles formed aggregates. Values of D were measured from the remaining nonaggregated particles.

probe did not vary appreciably over the erosion period, suggesting that the transport pathway was predominantly through the solid polymer. This conclusion is also supported by the very low orders of magnitude of measured D and the LSCM micrograph of PLGA microparticles immersed in probe solution (Figure 3). The probe emission from microparticles at a given position coordinate was very homogeneous. In contrast, pore diffusion is expected to yield heterogeneous emission, which was observed in control experiments with various fluorescent probes conjugated to dextran during uptake in the same PLGA microparticles used in this study (data not shown). The apparent partition coefficient of bodipy in PLGA/PBST was determined as 20 ± 2 (mean \pm SD, $n = 3$, independent of probe concentration), demonstrating this probe partitions strongly in PLGA. Therefore, the small probe size (MW = 292.1), the partitioning ability of the probe in the polymer, and the low pore connectivity in the polymer matrix are likely the primary causes of the apparent polymer diffusion control of bodipy.

PLGA microparticles are very important vehicles for protein and polypeptide delivery.^{3,35,36} Whereas protein release from PLGA microparticles is typically controlled by polymer erosion and diffusion in aqueous pores,^{35,36} the transport of water-soluble PLGA degradation products may in fact be controlled by polymer diffusion like bodipy. These acidic species (e.g., lactic/glycolic acids and their oligomers) are important factors determining the polymer erosion and formation of water-filled pores, through which hydrophilic macromolecules are released. The diffusion of PLGA degradation products also affects the acidic microenvironment inside PLGA microparticles, which is regarded as a primary culprit for protein instability in PLGA.^{37,38} Therefore, measurement of diffusion of small probes in PLGA could be invaluable for the understanding and modeling of polymer degradation, protein stability, and release from PLGA microparticles.

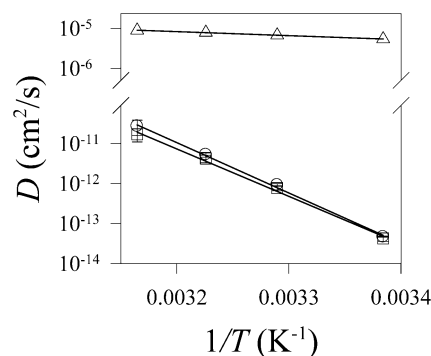


Figure 7. Temperature dependence of the bodipy diffusion coefficients (log scale, mean \pm SD, $n = 10$) in blank (○) and protein-containing (□) PLGA microparticles, as measured by confocal microscopy. The bodipy diffusion coefficients in water (Δ) were calculated by the Wilke–Chang estimation method. The trend lines have $R^2 > 0.995$.

In Figure 6 is displayed the diffusion coefficients of bodipy in BSA-encapsulated PLGA microparticles with or without MgCO₃, an insoluble basic excipient for neutralizing the acidic pH environment inside PLGA microparticles.^{3,38} In contrast to the blank formulation, probe diffusion in the protein-loaded microparticles was initially rapid declining to a minimum after ~2 weeks followed by an increase after 3 weeks. Moreover, protein-encapsulated microparticles at the initial time point (designated in Figure 6 by a “**”) exhibited a deformed irregular shape and heterogeneous probe distribution (data not shown). The heterogeneous probe distribution was likely caused by pores existing on the surface of PLGA microparticles during the initial incubation, which gave the highly variable values of D and poor fits to the diffusion model at this initial point ($R^2 > 0.77$). We have recently shown that over the first few days of incubation similar pores observed in peptide-loaded PLGA microparticles close by spontaneous polymer rearrangements.³⁹

At the end of the incubation of BSA-encapsulated microparticles an increased number and size of isolated pores were observed (data not shown), which may have contributed to the higher D (Figure 6) by advancing the diffusion front. Fits to (1) at later time points (24 days, designated in Figure 6 by a “*”) were also less desirable ($R^2 > 0.84$) (compared to the remaining time points which were excellent ($R^2 > 0.91$)). We have reported that encapsulation of protein and base greatly enhances water uptake of PLGA.^{37,38} The equivalent or lower values of D in high water content microparticles with protein (Figure 6) relative to low water content blank microparticles (Figure 5) is consistent again with primarily polymer diffusion control as opposed to diffusion through a pore network.^{37,38}

Temperature Dependence of Bodipy Diffusion Coefficients in PLGA Microparticles. To provide more definitive evidence of polymer diffusion control of bodipy, D was measured as a function of temperature after a 5 day preincubation of the microparticles with or without encapsulated protein at 37 °C in PBST. If pore diffusion were controlling, the measured $D(T)$ would be expected to vary in a similar manner as the aqueous diffusion coefficient of bodipy. As seen in Figure 7 (presented as an Arrhenius plot), a large variation in D in the blank microparticles was observed, e.g., from $D = 4.6 \times 10^{-14}$ cm²/s at 22.5 °C ($1/T = 0.00338$ K⁻¹) to $D = 2.7 \times 10^{-11}$ cm²/s at 43.0 °C ($1/T = 0.00317$ K⁻¹). The diffusion of bodipy in the 4 °C sample was so slow

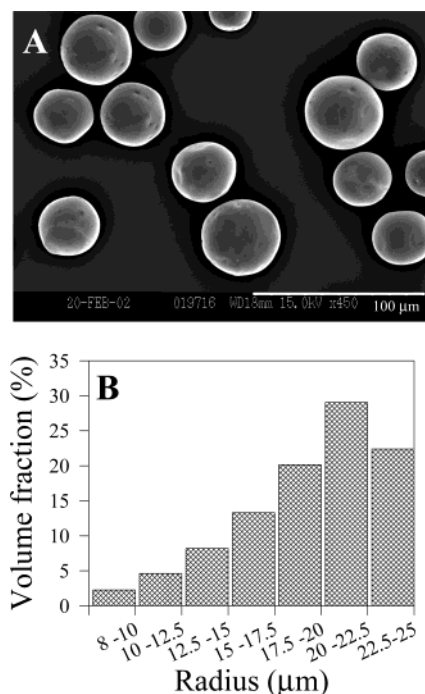


Figure 8. Scanning electron micrograph of probe-containing PLGA microparticles used for the release study (A) and the corresponding size distribution of the microparticles (B).

that significant probe concentration gradients could not be observed after 10 days of probe incubation, which prohibited determination of D . Also shown in the figure, addition of the pore-forming protein and basic additive (MgCO_3) to the polymer preparation did not significantly affect the measured D in the 5 day eroded microparticles. By contrast, the bodipy diffusion coefficient in water, determined by the well-known Wilke–Chang method, varied little with temperature (Figure 7). Although pore structure in PLGA microparticles changes with time, this process is relatively slow, especially after the polymer has been fully hydrated.³⁹ Therefore, we expect that the porosity and pore structure in the microparticles did not significantly change during the short equilibrium and uptake period (<6 h) at the various temperatures selected. Since the temperature dependence of bodipy diffusion in water was much less than that in PLGA microparticles, and the pore-forming substances (BSA, MgCO_3) did not significantly change D , the absence of a significant pore diffusion pathway is confirmed. The calculation of apparent activation energy for diffusion in blank and protein containing microparticles yielded values of 58 and 54 kcal/mol, respectively. This strong temperature-dependent polymer diffusion has also been found in other systems.⁴⁰

Predicting Bodipy Release from PLGA Microparticles. A small amount of bodipy was encapsulated into PLGA microparticles by using the same encapsulation conditions previously used for blank microparticles. The encapsulation efficiency of bodipy was $23.8 \pm 0.4\%$ with a corresponding loading of 0.67 ± 0.01 ng/mg. In Figure 8, morphology and size distribution of probe-encapsulated PLGA microparticles are displayed. The number- and volume-average radii were $17 \mu\text{m}$ and $19 \mu\text{m}$, respectively. Microparticles were spherical with the same morphology as those prepared without the probe in the uptake experiment. The time-averaged D determined for blank microparticles at 0, 1, and 3 days (7.9

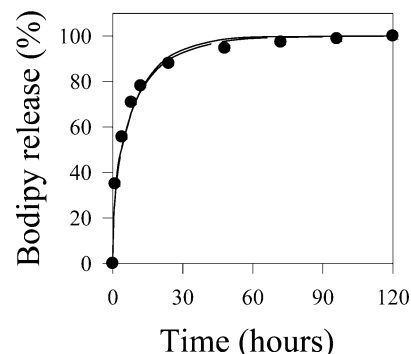


Figure 9. Measured (symbol) and predicted (—, prediction 1 from (3), ---, prediction 2 from (4)) probe release from PLGA microparticles. Symbols represent mean ($n = 3$), and standard deviations were smaller than symbols.

$\times 10^{-12} \text{ cm}^2/\text{s}$) was used to predict the bodipy release from PLGA microparticles. In the first prediction, the volume average radius ($a = 19 \mu\text{m}$) was used together with (3). In the second prediction, the heterogeneity of the size distribution was taken into account according to (4). The predicting curves are shown together with the normalized release data in Figure 9. The excellent predictions demonstrate the accuracy of the LSCM measurement. The negligible difference between predicted curves 1 and 2 is attributed to the narrow size distribution of microparticles used for the release experiment.

Conclusions

LSCM was used to measure the diffusion coefficient of a small hydrophobic molecule, bodipy, in PLGA microparticles. This method is simple, nondestructive and can be used to study the diffusion inside a single particle. The measured diffusion coefficients in blank or protein encapsulated PLGA microparticles were strongly temperature-dependent and were in the range of $(3\text{--}24) \times 10^{-12} \text{ cm}^2/\text{s}$ at 37°C . The transport of bodipy in PLGA microparticles is controlled by diffusion in the polymer phase. The release of bodipy from PLGA microparticles was well predicted by the measured diffusion coefficient in blank microparticles.

Acknowledgment. The authors thank Mr. Bruce Donohoe at Microscopy and Image Analysis Laboratory at the University of Michigan for training and help with confocal microscope. The authors thank Dr. Donald W. Schwendeman of Rensselaer Polytechnic Institute for his mathematical advice. The scanning electron microscope used in this study was funded in part by National Science Foundation Grant EAR-9628196. This research was supported by NIH HL 68345.

References and Notes

- (1) Schwendeman, S. P. *Crit. Rev. Ther. Drug Carrier Syst.* **2002**, *19*, 73–98.
- (2) Cui, C.; Schwendeman, S. P. *Macromolecules* **2001**, *34*, 8426–8433.
- (3) Zhu, G.; Mallery, S. R.; Schwendeman, S. P. *Nat. Biotechnol.* **2000**, *18*, 52–57.
- (4) Anderson, J. M.; Shive, M. S. *Adv. Drug Del. Rev.* **1997**, *28*, 5–24.
- (5) Shah, S. S.; Cha, Y.; Pitt, C. G. *J. Controlled Release* **1992**, *18*, 261–270.
- (6) Cleland, J. L.; Jones, A. J. *Pharm. Res.* **1996**, *13*, 1464–1475.
- (7) Kappy, M.; Stuart, T.; Perelman, A.; Clemons, R. *J. Clin. Endocrin. Metabol.* **1989**, *69*, 1087–1089.

- (8) Charlier, A.; Leclerc, B.; Couarraze, G. *Int. J. Pharm.* **2000**, *200*, 115–120.
- (9) Siepmann, J.; Gopferich, A. *Adv. Drug Del. Rev.* **2001**, *48*, 229–247.
- (10) Batycky, R. P.; Hanes, J.; Langer, R.; Edwards, D. A. *J. Pharm. Sci.* **1997**, *86*, 1464–1477.
- (11) Li, S.; Garreau, H.; Vert, M. *J. Mater. Sci. Mater. Med.* **1990**, *1*, 123–130.
- (12) Li, S.; Garreau, H.; Vert, M. *J. Mater. Sci. Mater. Med.* **1990**, *1*, 131–139.
- (13) Tracy, M. A.; Ward, K. L.; Firouzabadian, L.; Wang, Y.; Dong, N.; Qian, R.; Zhang, Y. *Biomaterials* **1999**, *20*, 1057–1062.
- (14) Schwendeman, S. P.; Costantino, H. R.; Gupta, R. K.; Langer, R. In *Controlled Drug Delivery: Challenges and Strategies*; Park, K., Ed.; American Chemical Society: Washington, DC, 1997; pp 229–267.
- (15) Crank, J.; Park, G. S. In *Diffusion in Polymers*; Crank, J., Park, G. S., Eds.; Academic Press: New York, 1968; pp 1–39.
- (16) Westrin, B. A.; Axelsson, A.; Zacchi, G. *J. Controlled Release* **1994**, *30*, 189–199.
- (17) Kou, J. H.; Amidon, G. L.; Lee, P. I. *Pharm. Res.* **1988**, *5*, 592–597.
- (18) Yoon, J.; Jung, H.; Kim, M.; Park, E. *J. Appl. Polym. Sci.* **2000**, *77*, 1716–1722.
- (19) Mavituna, F.; Park, J. M. *Chem. Eng. J.* **1987**, *34*, B1–B5.
- (20) Stilbs, P. *Prog. NMR Spectrosc.* **1987**, *19*, 1–45.
- (21) Fang, L.; Brown, W. *Macromolecules* **1990**, *23*, 3284–3290.
- (22) Cutts, L. S.; Hibberd, S.; Adler, J.; Davies, M. C.; Melia, C. D. *J. Controlled Release* **1996**, *42*, 115–124.
- (23) McFarland, E. G.; Michielsen, S.; Carr, W. W. *Appl. Spectrosc.* **2001**, *55*, 481–489.
- (24) Meyvis, T. K. L.; De Smedt, S. C.; Oostveldt, P. V.; Demeester, J. *Pharm. Res.* **1999**, *16*, 1153–1162.
- (25) Song, Y.; Srinivasarao, M.; Tonelli, A.; Balik, C. M.; McGregor, R. *Macromolecules* **2000**, *33*, 4478–4485.
- (26) Kim, H.; Hayashi, M.; Nakatani, K.; Kitamura, N.; Sasaki, K.; Hotta, J.; Masuhara, H. *Anal. Chem.* **1996**, *68*, 409–414.
- (27) De Smedt, S. C.; Meyvis, T. K. L.; Demeester, J. *Macromolecules* **1997**, *30*, 4863–4870.
- (28) Burke, M. D.; Park, J. O.; Srinivasarao, M.; Khan, S. A. *Macromolecules* **2000**, *33*, 7500–7507.
- (29) Crank, J. In *The Mathematics of Diffusion*; Crank, J., Ed.; Clarendon Press: Oxford, 1975; pp 89–103.
- (30) Pitt, C. G.; Jeffcoat, A. R.; Zweidinger, R. A.; Schindler, A. *J. Biomed. Mater. Res.* **1979**, *13*, 497–507.
- (31) Karolin, J.; Johansson, L. B.-A.; Strandberg, L.; Ny, T. *J. Am. Chem. Soc.* **1994**, *116*, 7801–7806.
- (32) Oostveldt, P. V.; Bauwens, S. *J. Microsc.* **1990**, *158*, 121–132.
- (33) Sandison, D. R.; Williams, R. M.; Wells, K. S.; Strickler, J.; Webb, W. W. In *Handbook of Biological Confocal Microscopy*; Pawley, J. B., Ed.; Plenum Press: New York, 1995; pp 39–53.
- (34) Heertje, I.; Nederlof, J.; Hendrickx, H. A. C. M.; Lucassen-Reynders, E. H. *Food Struct.* **1990**, *9*, 305–316.
- (35) Pitt, C. G. *Int. J. Pharm.* **1990**, *59*, 173–196.
- (36) Siegel, R. A.; Langer, R. *Pharm. Res.* **1984**, *1*, 2–10.
- (37) Zhu, G.; Schwendeman, S. P. *Pharm. Res.* **2000**, *17*, 351–357.
- (38) Kang, J.; Schwendeman, S. P. *Biomaterials* **2002**, *23*, 239–245.
- (39) Wang, J.; Wang, B. M.; Schwendeman, S. P. *J. Controlled Release* **2002**, *82*, 289–307.
- (40) Takeuchi, H. *J. Chem. Phys.* **1990**, *92*, 5643–5652.

MA021036+